Plasmonics Hot Paper

International Edition: DOI: 10.1002/anie.201503384
German Edition: DOI: 10.1002/ange.201503384

Black Gold: Plasmonic Colloidosomes with Broadband Absorption Self-Assembled from Monodispersed Gold Nanospheres by Using a Reverse Emulsion System**

Dilong Liu, Fei Zhou, Cuncheng Li, Tao Zhang, Honghua Zhang, Weiping Cai, and Yue Li**

Abstract: *A facile approach for the fabrication of novel black plasmonic colloidosomes assembled from Au nanospheres is developed by an emulsion-templating strategy. This self-assembly process is based on a new reverse water-in-1-butanol emulsion system, in which the water emulsion droplets can dissolve into 1-butanol (oil) phase at an appropriate rate. These Au colloidosomes possess hexagonal close-packed multilayer shells and show a low reflectivity and intense broadband absorption owing to the strong interparticle plasmonic coupling, which is further investigated by a finite-difference time-domain method. This method is universal and is suitable for self-assembly of different noble-metal nanoparticles into different colloidosomes. These colloidosomes have important applications in photothermal therapy, biosensors, and drug delivery.*

Plasmonic metal nanostructures have particular light–matter interactions, known as the localized surface plasmon resonance (LSPR).[1] Since the complex structures self-assembled by plasmonic nanoparticles (NPs) would induce the near-field coupling of surface plasmons between neighboring NPs,[2] novel optical properties might emerged. For instance, when spherical Au NPs were self-assembled into two-dimensional ordered arrays, a golden color in reflection and an associated purple color in transmission can be observed because of a collective plasmon resonance mode existing in Au NP arrays.[3] For three-dimensional (3D) structures, the spherical plasmonic vesicles composed of amphiphilic Au NPs show a near-infrared absorption induced by interparticle plasmonic coupling between adjacent Au NPs, which have important applications in photothermal therapy,[4] bioimaging, and targeted drug delivery.[5]

Plasmonic vesicles (PVs), as the promising theranostic platform for biomedical applications, have drawn more and more attention.[6] A well-used method for the fabrication of PVs is the polymerization-induced self-assembly of Au NPs. Usually, a copolymer with amphiphilic ligands has been decorated with Au NPs to make them form PVs, such as semi-fluorinated ligands[7] and terpyridine thiol.[8] However, these Au NPs are embedded into a cross-linked polymer, which seriously affects their further applications. Further significant advances have been made in the development of pH-responsive PVs self-assembled from SERS (surface-enhanced Raman scattering)-encoded Au NPs for drug delivery.[5a] Nevertheless, the Au NPs employed in PVs have a poor monodispersity and they are irregularly cross-linked on the shells of PVs, which are unfavorable for the enhancement of interparticle plasmonic coupling.

Recently, colloidosomes composed of hexagonal close-packed (HCP) colloidal particles, which are similar to PVs, can be fabricated by self-assembly using the principle of the total interface energy minimum.[9] The cross-linking of the polymer molecules on the colloidal particles is not needed for such assembly of colloidosomes.[10] The structures of colloidosomes render them to be very suitable for strong interparticle plasmonic coupling between adjacent units if Au NPs are used.[11] Deng et al. reported the formation of Au colloidosomes by a hard-templating method.[12] There might be an opportunity to achieve an aggregate with stronger plasmonic coupling by self-assembling larger Au NPs into colloidosomes based on a simple soft-templating method. However, up to now, there are no relative attempts found in the literature for the fabrication of colloidosomes composed of monodispersed Au NPs and the investigation of plasmonic coupling between adjacent Au NPs.

Herein, we develop a facile emulsion-templating approach to fabricate 3D plasmonic colloidosomes (PCs) composed of HCP Au nanospheres based on a new reverse (water-in-1-butanol) emulsion system. The Au colloidosomes display a stronger plasmonic coupling effect with broadband absorption, and hence have a black color intrinsically, so they are called black gold. These Au PCs possess a multilayer shell of HCP monodispersed Au nanospheres and show a good

[*] D. Liu,[+] Dr. F. Zhou,[+] H. Zhang, Prof. W. Cai, Prof. Y. Li
Key Lab of Materials Physics
Anhui Key Lab of Nanomaterials and Nanotechnology
Institute of Solid State Physics
Chinese Academy of Sciences, Hefei 230031 (P.R. China)
E-mail: yueli@issp.ac.cn
D. Liu,[+] H. Zhang, Prof. Y. Li
University of Science and Technology of China
Hefei 230026 (P.R. China)
C. Li, T. Zhang
School of Chemistry and Chemical Engineering
University of Jinan, Jinan 250022, Shandong (P.R. China)
E-mail: chm_licc@ujn.edu.cn
[+] These authors contributed equally to this work.

[**] The authors acknowledge the financial support from the National Basic Research Program of China (grant number 2012CB932303), Recruitment Program of Global Experts (C), Natural Science Foundation of China (grant numbers 51371165 and 11204317), Cross-disciplinary Collaborative Teams Program in CAS, the CAS/SAFEA International Partnership Program for Creative Research Teams and Anhui Provincial Natural Science Foundation (grant number 1508085JGD07). C.C. Li as a Taishan Scholar Endowed Professor acknowledges the supports from Shandong province and UJN.

Supporting information for this article is available on the WWW under http://dx.doi.org/10.1002/anie.201503384.

mechanical stability relative to the conventional PVs.[6a] This strategy is universal and it is also suitable for nonspherical noble-metal NPs, such as Au nanooctahedra and Au–Ag heterogeneous nanorods to self-assemble them into metal PCs. To the best of our knowledge, this is first report to fabricate PCs composed of uniform HCP noble-metal NPs. The presented strategy will pave a way to achieve noble-metal superstructures for biosensors, drug delivery, photothermal therapy, optical microcavity, and microreaction platforms.

Monodispersed Au nanospheres were prepared by a modified polyol route and followed by a chemical etching process, as we previously reported.[13] Au NPs with an average size of 98 ± 2.6 nm are used as building blocks for the further fabrication, as shown in Figure S1 in the Supporting Information. Figure 1 a–f shows the FESEM and scanning TEM (STEM) images of the plasmonic colloidosomes, which were self-assembled from Au NPs (see the Supporting Information for experimental details). The obtained PCs have a size distribution ranging from 0.5 to 5 μm (Figure 1 a). Most of them have intact spherical shapes and only a few of them have chipped edges. Figure 1 b shows intact PCs with perfect spherical structures assembled with HCP Au NPs. Such HCP arrangement of Au NPs is also observed from PCs with different sizes in diameter (Figure S2). An STEM image confirms that the internal structure of the obtained PC is hollow (Figure 1 c). The shells of PCs contain several HCP ordering patches of NPs, some boundaries, and packing-defects could be observed on their surfaces. Previous studies[9c,14] demonstrated that the presence of packing-defects was essentially required for the topological constraints on curved surfaces. Figure 1 d–f shows some partially broken PCs with different sizes, further indicating the formation of hollow PCs. A PC with larger size (i.e. 5 μm) consisted of a uniform five-layered shell (Figure 1 d), and this shell was neatly and layer by layer constructed using the NPs (Figure 1 e). With decreasing size of the PC, the layer number also decreased. The PC with a size of about 2 μm was composed of a bilayer shell (Figure 1 f). When the concentration of the Au NP suspension keeps a certain value, the layer number of a PC shell will scale approximately with its radius, as we analyzed in the Supporting Information. This indicates that with increasing size of the PC, its layer number will also increase. Moreover, a higher mechanical stability can be achieved for these multilayer PCs compared to conventional monolayered colloidosomes and PVs. Peyratout and Dähne showed that the mechanical properties of a shell can be reinforced simply by increasing the number of the deposited layers.[15] The much higher mechanical stability would arise from the increased interaction between the adjacent layers and the HCP Au NPs in the shell.

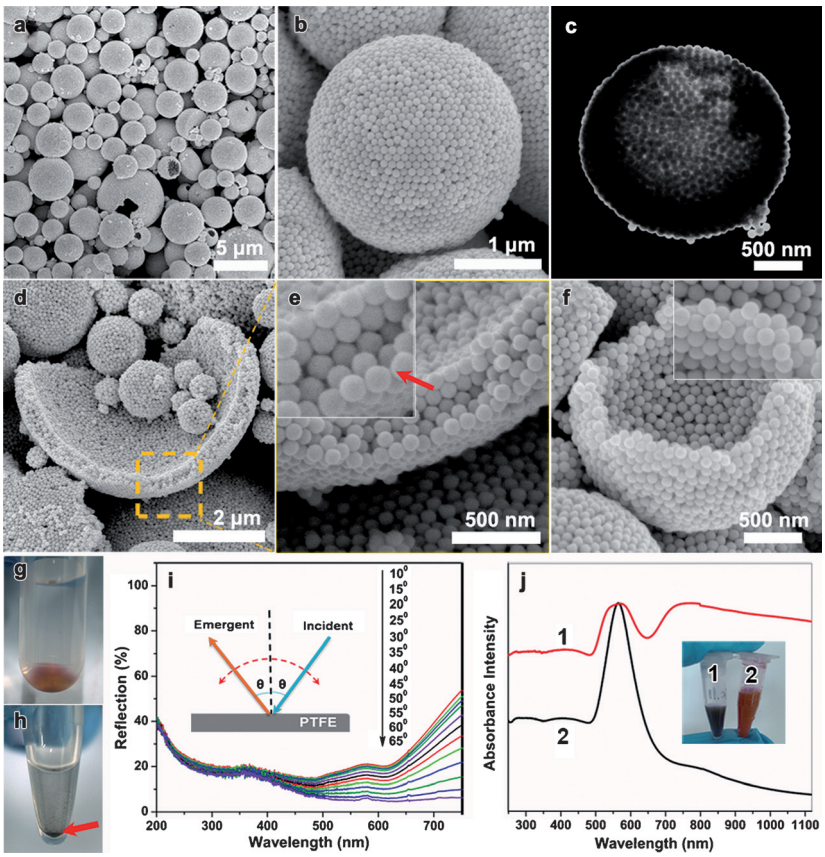

Figure 1. a,b) SEM images of the self-assembled Au PCs. c) Scanning-TEM image of single Au PC. d–f) SEM images of the broken Au PCs with different size. e) The high-magnification SEM image marked in the frame of (d). Insets in (e) and (f) show their corresponding high-magnification SEM images, respectively. g,h) Photos of red colloidal Au NPs and black PCs settled on the bottom of tubes, respectively. i) Reflection spectra of the PCs deposited on the PTFE substrate measured at the angle ranging from 10–65° with a test step of 5°. The inset in (i) shows the scheme of upper reflection. j) The absorption spectra of black Au PCs (curve 1) and Au NPs (curve 2) suspended in 1-butanol, respectively. The inset in (j) shows the corresponding photograph of PCs (1) and colloidal Au NPs (2) suspended in 1-butanol.

Normally, Au NPs deposited by centrifugation at the bottom of a tube appear brick red (Figure 1 g). But the obtained PCs self-assembled from the Au NPs appear dark black (Figure 1 h). Figure 1 i shows the reflection spectra of the Au PCs deposited on a polytetrafluoroethylene (PTFE) substrate measured at an upper reflection model. The reflectivity of the Au PCs is lower than 20% in most of the UV/Vis region at different incident directions, indicating that most of the incident light has been absorbed by the PCs. Figure 1 j shows the absorption spectra of the obtained PCs and Au NPs. The Au NPs dispersed in 1-butanol have one LSPR peak centered at 564 nm (curve 2, Figure 1 j). But for Au PCs (curve 1, Figure 1 j), the LSPR peak centered at 564 nm diminished, and a broad near-infrared (NIR) plasmon absorption band appeared because of the strong plasmonic coupling among the Au NPs in the PC shell.[6a] Additionally, a whole broad absorption can also be observed in optical absorption spectrum of PCs. Therefore, the obtained PCs demonstrate dark black color.

In the self-assembling process of colloidosomes, there are two specific requirements for the reverse (water in oil) system.[16] One is that the water phase should be able to dissolve in the oil phase completely at an appropriate rate. Another one is that the building blocks should be adsorbed on the water/oil interfaces rapidly. Therefore, it is crucial to select suitable reverse emulsion system to self-assemble different colloidosomes. Herein, we employed the water-in-1-butanol system for the first time, which completely meets the above-mentioned requirements, because the solubility of water in 1-butanol has an appropriate value, ca. 20.4 % w/w (25 °C).[17] A key advantage of this system to fabricate PCs is that such self-assembly can avoid the introduction of complex stabilization process to lock the NPs together.

In this work, an appropriate concentration of Au NPs in the starting colloidal solution is critical to form the desired PCs composed of HCP NPs. At a low concentration of the Au NPs (i.e. 10 wt %), the yield of the Au PCs showed good spherical structures but with randomly packed Au NPs on the shells (Figure S3 a,b). With increasing the concentration to 16 wt %, the PCs exhibited better spherical structures and were composed of HCP Au NPs on the shells (Figure S3 c,d). When the concentration was very high (i.e. 30 wt. %), lots of Au NPs dispersed in the aqueous phase would aggregate together, causing the disorganized sediment of Au NPs in the products (Figure S3 e,f). This morphological evolution of the PCs is closely related to the changes in the concentration of the Au NP suspension. For a low concentration, the quick dissolution of the water emulsion droplets will result in an insufficient feedstock of Au NPs at the W/O interface, forming poorly ordered NPs on the shell as the interface shrinks. In contrast, a high concentration of Au NPs accelerates the coagulation process which initiates the formation of the colloidal suspension. Only an appropriate concentration that effectively competed with the rate of dissolution is essential for the formation of PC shells with HCP arrangement of the Au NPs.

Moreover, the pretreatment of pristine Au NPs with 1-butanol additionally influenced the formation of well-ordered PCs. The use of Au NPs pretreated with 1-butanol resulted in an HCP arrangement on the PC shell (Figure S3 c,d). In contrast, these Au NPs without the 1-butanol pretreatment tend to form a rough and poorly ordered shell of PCs (Figure S3 g,h). By such pretreatment, the adsorption rate of the NPs at the water/1-butanol interface was much improved, which is likely induced by the competitive adsorption of tiny amounts of 1-butanol molecules on the surface of the NPs which slightly decreased the surface charge.[18]

Generally, there is a key distinction between the reverse water-in-butanol system and the traditional immiscible emulsion one. In the latter system, the colloidosomes with only monolayer NPs were formed by self-assembly at the interface between the two immiscible liquids.[9a] But the resultant colloidosomes in our approach consisted of a multilayered shell, which is also distinct from the multilayer colloidosomes formed by the double emulsion system.[19] Here, the formation of multilayered shells can be attributed to the appropriate dissolubility of the water droplets in the 1-butanol phase at the interface of water and butanol, as confirmed by some fluorescence micrographs to demonstrate the diffusion of water into butanol by introducing fluorescent dyes (FITC) into the water phase (Figure S4). They clearly show that the FITC-labeled water phase gradually diffused into the 1-butanol phase at an appropriate rate. When 1-butanol was replaced by an immiscible solution, that is, toluene and n-hexane, the PC structures did not form because of the rapid coalescence of the water droplets. When it was replaced by a miscible solution, that is, ethanol and isopropanol, the Au NPs ended up with well-dispersed states in the solvents and the colloidosomes could not form at all. The above facts further confirmed that the appropriate dissolubility of water droplets into the 1-butanol phase at the W/O interface plays a key role in the formation of PCs with multilayered NP shells.

Figure 2 shows the self-assembling mechanism for the fabrication of PCs with multilayered shells. After ultrasonic dispersion, the water emulsion droplets containing the Au NPs were suspended in 1-butanol. These Au NPs spontaneously absorbed at the emulsion interface, driven by the minimization of the total interfacial free energy[9e,20] and hence a single layer of NPs was trapped at the water/butanol interface (Figure 2 a). After a while, the appropriate dissolubility of water in 1-butanol led to a small quantity of water diffusing into the surrounding oil environment at the interface, forcing the interfacial curvature area to shrink inward. When the interfacial area decreased, the trapped layer of the NPs was compressed. Once the Au NPs were closely packed on the entire droplet surface, they jammed into the solid and close-packed shell (Figure 2 b). As the diffusion of water into butanol continued, the inner NPs in the water droplet met the new interface between the first layer shell and water, and the NPs preferentially resided onto the inside interstice of the HCP shell. In the same way, an HCP shell with two or several stacked layers finally formed until all Au NPs were incorporated into the shell. As the NPs of the water droplet were exhausted, an ordered HCP multilayer structure was obtained (Figure 2 c). Once the self-assembling process was finished

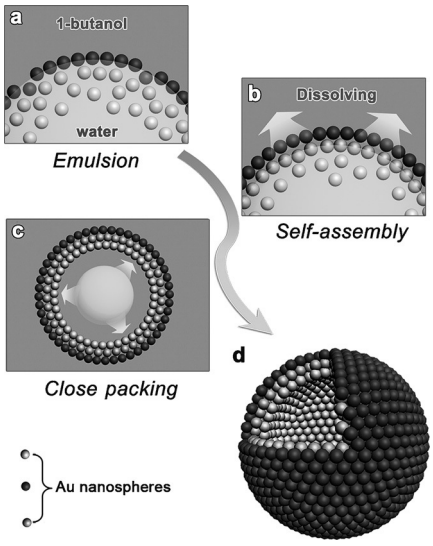

Figure 2. Self-assembling mechanism of multilayered PCs.

and the PCs were formed, the attractive van der Waals forces between neighboring Au NPs in the shell played a critical role in keeping their structures intact.[9a,16] PCs with HCP multilayered shells finally settled down on the bottom of the container as the water droplets dissolved completely.

The fabrication of PCs using different sizes of Au nanospheres (54, 62, 90, and 115 nm in diameter) was also investigated. Using the presented strategy, a series of similar PCs composed of Au NPs with different sizes could be fabricated by self-assembly, as shown in Figure S5. Besides spherical Au NPs, other noble-metal NPs with non-spherical shapes, that is, Au nano-octahedra, and Au–Ag heterogeneous nanorods were also used to fabricate interesting PCs, as shown in Figures S6 and S7. These resulting PCs also have a dark-black color. Both of them had a spherical shape and a multilayered shell structure, which agrees well with the proposed mechanism. Therefore, this reverse emulsion system is capable of adopting a variety of building block sizes and shapes for the fabrication of PCs.

We discuss the origin of the strong broadband absorption of as-prepared PCs. By using the finite-difference time domain (FDTD) method, we calculated the absorbance spectra of the PC array, as shown in Figure 3a (the black curve). The refractive index of Au is obtained from Palik.[21] The diameter of the PCs is 500 nm, and the diameter of the Au nanospheres is 60 nm. The results indicate that, for wavelengths from 400 to 1000 nm, the PCs show strong absorption of the incident light. For comparison, we also calculated the refractive spectra of a four-layered planar nanosphere array (the red curve in Figure 3a) and there is an absorption peak at 810 nm. However, for other wavelengths, the absorption is weak. To understand this, we further calculated the electric field near the PC array (Figure 3b) and the planar array (Figure 3c) using a non-resonant wavelength; here we choose 700 nm. We can find that in the PC array the maximum electric field enhancement factor is much larger than that of the planar array. Since the larger electric field indicates stronger optical absorption, the optical absorption of the PC is larger than the planar arrays. For other wavelengths, the main electric field would be confined at different positions. The dipolar plasmon resonances and the plasmonic near-field coupling between the adjacent NPs can provide resonant light coupling and absorption at different wavelength ranges, which therefore produce a broadband light absorption.[22] Meanwhile, strong near-field coupling between non-close-packed plasmonic NPs with a small quantity existing in PCs can introduce a broadened optical field confinement.[23] Moreover, curved surfaces[24] and a half-shell[25] on dielectric colloids can also enhance the optical absorption.

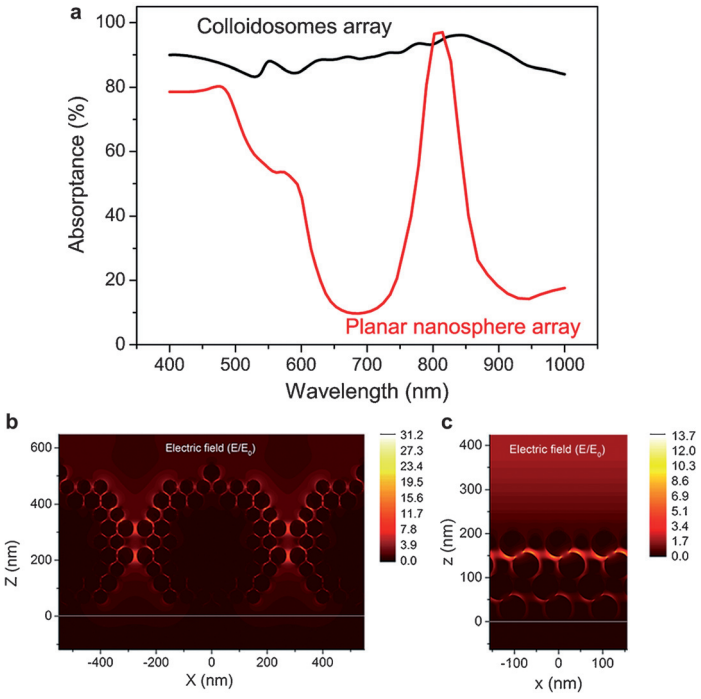

Figure 3. a) The calculated absorbance spectra of the PC array (black curve) and the four-layered planar NP array (red curve) by the FDTD method. b,c) Simulated electric-field amplitude distribution of the PC array (b) and planar NP array (c), respectively.

In summary, we developed a facile and rapid emulsion-templating approach for the fabrication of Au PCs based on a reverse emulsion system. Unlike conventional emulsion approaches, the presented reverse emulsion strategy can be used for the formation of PCs with an HCP multilayered shell, which can be attributed to the dissolution of the water droplets into 1-butanol at an appropriate rate. These PCs show a low reflectivity and strong broadband absorption because of the strong interparticle plasmonic coupling, hence leading to a dark-black color. The origin of the strong broadband absorption of as-prepared PCs was also investigated by FDTD method. The mechanism has been reasonably presented to understand the formation of multilayered shells. This reverse emulsion system is universal for fabricating various colloidosomes. These novel black PCs provide a new category of superstructures which might have important applications in biosensors, photothermal therapy, drug delivery, and microreaction platforms.

Keywords: colloidosomes · gold · plasmonics · reverse emulsion systems · self-assembly

How to cite: *Angew. Chem. Int. Ed.* **2015**, *54*, 9596–9600
Angew. Chem. **2015**, *127*, 9732–9736

[1] K. A. Willets, R. P. Van Duyne, *Annu. Rev. Phys. Chem.* **2007**, *58*, 267–297.
[2] a) A. Chen, A. E. DePrince, A. Demortière, A. Joshi-Imre, E. V. Shevchenko, S. K. Gray, U. Welp, V. K. Vlasko-Vlasov, *Small* **2011**, *7*, 2365–2371; b) Y. Liu, X. Han, L. He, Y. Yin, *Angew. Chem. Int. Ed.* **2012**, *51*, 6373–6377; *Angew. Chem.* **2012**, *124*, 6479–6483.
[3] a) T. P. Bigioni, X. M. Lin, T. T. Nguyen, E. I. Corwin, T. A. Witten, H. M. Jaeger, *Nat. Mater.* **2006**, *5*, 265–270; b) M. H. Lin, H. Y. Chen, S. Gwo, *J. Am. Chem. Soc.* **2010**, *132*, 11259–11263.
[4] a) P. Huang, J. Lin, W. Li, P. Rong, Z. Wang, S. Wang, X. Wang, X. Sun, M. Aronova, G. Niu, *Angew. Chem. Int. Ed.* **2013**, *52*, 13958–13964; *Angew. Chem.* **2013**, *125*, 14208–14214; b) J. Lin, S. Wang, P. Huang, Z. Wang, S. Chen, G. Niu, W. Li, J. He, D. Cui, G. Lu, *ACS Nano* **2013**, *7*, 5320–5329.

[5] a) J. Song, J. Zhou, H. Duan, *J. Am. Chem. Soc.* **2012**, *134*, 13458 – 13469; b) K. Niikura, N. Iyo, Y. Matsuo, H. Mitomo, K. Ijiro, *ACS Appl. Mater. Interfaces* **2013**, *5*, 3900 – 3907; c) J. Song, L. Pu, J. Zhou, B. Duan, H. Duan, *ACS Nano* **2013**, *7*, 9947 – 9960.
[6] a) J. Song, L. Cheng, A. Liu, J. Yin, M. Kuang, H. Duan, *J. Am. Chem. Soc.* **2011**, *133*, 10760 – 10763; b) Y. Wang, B. Yan, L. Chen, *Chem. Rev.* **2012**, *112-112*, 1391 – 1428; c) A. E. Vasdekis, E. A. Scott, S. Roke, J. A. Hubbell, D. Psaltis, *Annu. Rev. Mater. Res.* **2013**, *43*, 283 – 305.
[7] K. Niikura, N. Iyo, T. Higuchi, T. Nishio, H. Jinnai, N. Fujitani, K. Ijiro, *J. Am. Chem. Soc.* **2012**, *134*, 7632 – 7635.
[8] D. Patra, N. Malvankar, E. Chin, M. Tuominen, Z. Gu, V. M. Rotello, *Small* **2010**, *6*, 1402 – 1405.
[9] a) A. Dinsmore, M. F. Hsu, M. Nikolaides, M. Marquez, A. Bausch, D. Weitz, *Science* **2002**, *298*, 1006 – 1009; b) M. Pang, A. J. Cairns, Y. Liu, Y. Belmabkhout, H. C. Zeng, M. Eddaoudi, *J. Am. Chem. Soc.* **2013**, *135*, 10234 – 10237; c) X. W. Xu, X. M. Zhang, C. Liu, Y. L. Yang, J. W. Liu, H. P. Cong, C. H. Dong, X. F. Ren, S. H. Yu, *J. Am. Chem. Soc.* **2013**, *135*, 12928 – 12931; d) T. Bollhorst, S. Shahabi, K. Wörz, C. Petters, R. Dringen, M. Maas, K. Rezwan, *Angew. Chem. Int. Ed.* **2015**, *54*, 118 – 123; *Angew. Chem.* **2015**, *127*, 120 – 125; e) Z. Niu, J. He, T. P. Russell, Q. Wang, *Angew. Chem. Int. Ed.* **2010**, *49*, 10052 – 10066; *Angew. Chem.* **2010**, *122*, 10250 – 10265.
[10] A. D. Dinsmore, *Nat. Mater.* **2007**, *6*, 921 – 922.
[11] a) G. Bachelier, I. Russier-Antoine, E. Benichou, C. Jonin, N. Del Fatti, F. Vallée, P. F. Brevet, *Phys. Rev. Lett.* **2008**, *101*, 197401; b) K. Thyagarajan, J. r. m. Butet, O. J. Martin, *Nano Lett.* **2013**, *13*, 1847 – 1851.
[12] M. Liu, Q. Tian, Y. Li, B. You, A. Xu, Z. Deng, *Langmuir* **2015**, 31, 4589-4592.
[13] C. Li, K. L. Shuford, M. Chen, E. J. Lee, S. O. Cho, *ACS Nano* **2008**, *2*, 1760 – 1769.
[14] P. Lipowsky, M. J. Bowick, J. H. Meinke, D. R. Nelson, A. R. Bausch, *Nat. Mater.* **2005**, *4*, 407 – 411.
[15] C. S. Peyratout, L. Dähne, *Angew. Chem. Int. Ed.* **2004**, *43*, 3762 – 3783; *Angew. Chem.* **2004**, *116*, 3850 – 3872.
[16] O. Velev, K. Nagayama, *Langmuir* **1997**, *13*, 1856 – 1859.
[17] *Handbook of organic solvent properties* (ED.:I. Smallwood), Butterworth-Heinemann, **2012**.
[18] F. Reincke, S. G. Hickey, W. K. Kegel, D. Vanmaekelbergh, *Angew. Chem. Int. Ed.* **2004**, *43*, 458 – 462; *Angew. Chem.* **2004**, *116*, 464 – 468.
[19] J. S. Sander, A. R. Studart, *Soft matter* **2014**, *10*, 60 – 68.
[20] Z. Mao, H. Xu, D. Wang, *Adv. Funct. Mater.* **2010**, *20*, 1053 – 1074.
[21] *Handbook of Optical Constants of Solids* (Ed.: E. Palik), Academic, Orlando **1985**.
[22] a) Z. Liu, H. Shao, G. Liu, X. Liu, H. Zhou, Y. Hu, X. Zhang, Z. Cai, G. Gu, *Appl. Phys. Lett.* **2014**, *104*, 081116; b) Z. Liu, G. Liu, S. Huang, X. Liu, P. Pan, Y. Wang, G. Gu, *Sens. Actuators B* **2015**, *215*, 480 – 488.
[23] Z. Liu, Y. Nie, W. Yuan, X. Liu, S. Huang, J. Chen, H. Gao, G. Gu, G. Liu, *Nanotechnology* **2015**, *26*, 185701.
[24] W. R. Wei, M. L. Tsai, S. T. Ho, S. H. Tai, C. R. Ho, S. H. Tsai, C. W. Liu, R. J. Chung, J. H. He, *Nano Lett.* **2013**, *13*, 3658 – 3663.
[25] a) Z. Liu, J. Hang, J. Chen, Z. Yan, C. Tang, Z. Chen, P. Zhan, *Opt. Express* **2012**, *20*, 9215 – 9225; b) Z. Liu, P. Zhan, J. Chen, C. Tang, Z. Yan, Z. Chen, Z. Wang, *Opt. Express* **2013**, *21*, 3021 – 3030.

Received: April 19, 2015
Revised: May 16, 2015
Published online: June 25, 2015

